

Fly-Ash-Based Geopolymers: How the Addition of Recycled Glass or Red Mud Waste Influences the Structural and Mechanical Properties

N. Toniolo¹, G. Taveri², K. Hurler³, J.A. Roether⁴,
P. Ercole⁵, I. Dlouhý², A.R. Boccaccini^{*1}

¹Institute of Biomaterials, Department of Materials Science and Engineering,
University of Erlangen-Nuremberg, Cauerstrasse 6, 91058 Erlangen, Germany

²Institute of Physics of Materials, Czech Academy of Science, Žižkova 22, 616 62 Brno, Czech Republic

³Institute of Mineralogy, University of Erlangen-Nuremberg, Schlossgarten 5a, 91054 Erlangen, Germany

⁴Institute of Polymer Materials, University of Erlangen-Nuremberg, Martensstrasse 7, 91058 Erlangen, Germany

⁵Sasil S.p.a, Regione Dosso, 13862 Brusnengo BI, Italy

received July 7, 2017; received in revised form August 11, 2017; accepted August 27, 2017

Abstract

One of the main advantages of geopolymer technology is its capability to accommodate several types of waste that would otherwise be disposed of in landfills in the production of geopolymer materials. This study investigates the possibility of substituting proportions of fly ash, normally used for the synthesis of geopolymers, with recycled glass and red mud waste. Compressive and flexural strength testing, fracture toughness determination, SEM and FTIR analyses were performed. The results show that the compressive strength decreases as the amount of glass in the geopolymer increases; on the other hand, the addition of red mud seems to improve the mechanical behavior. Moreover, on substitution of fly ash with glass and red mud, the geopolymer demonstrates a similar performance in terms of fracture toughness and flexural strength properties. The results confirm that red mud and waste glass have the potential to partially replace fly ash in geopolymer synthesis, opening thus the possibility of using geopolymer technology to reuse such residues in technical materials.

Keywords: Geopolymers, fly ash, red mud, waste glass

1. Introduction

The term “geopolymer” was proposed by Davidovits in 1978 to identify a class of materials with a chemical composition similar to natural zeolite but with semi-amorphous instead of crystalline microstructure¹. A geopolymer is the product of inorganic polymerization in which an alkaline solution, usually sodium hydroxide or potassium hydroxide, reacts with a source of alumina and silica.

The chemical mechanism can be interpreted as the initial dissolution of aluminates and silicate and the subsequent formation of an aluminosilicate gel phase through the polycondensation between silicate solution and Al and Si complexes. The final structure is a three-dimensional network of Al₂O₃ and SiO₂ in tetrahedral coordination, linked through shared O atoms. The negative charge induced by tetrahedral aluminates is balanced by alkalis from the activating solution^{2, 3}.

Geopolymers were developed primarily as an ecofriendly and sustainable alternative to conventional cement-based construction materials⁴. It is indeed estimated that for each tonne of cement, nearly one tonne of CO₂ is emitted^{5, 6, 7}. Because of their attractive properties, besides for construction, geopolymers are being considered

for many other applications such as refractory adhesive for glass, ceramics, fire-resistant materials and high-tech lightweight structures^{8, 9, 10}.

The growing interest in geopolymers is mainly attributed to the ecofriendly and low-cost technology resulting from the low-temperature processing and the possibility to incorporate in the geopolymer network waste materials that are otherwise disposed of. Moreover, the incorporation of other materials, like fibers as reinforcement, could improve the flexural strength and fracture toughness of the resulting composite material¹¹. Fly ash (FA), a by-product of coal combustion in thermal power plants, is the most suitable waste material for geopolymerization because of its convenient aluminosilicate composition, worldwide availability and pozzolanic property¹². Other types of residues are also continuously investigated to fabricate geopolymers¹³.

In this study, red mud, a waste generated in alumina production, and recycled soda lime glass are investigated as addition to fly ash to synthesize geopolymers.

Red mud (RM) has high basicity and leaching potential owing to the large amount of alkali used in the alumina production process. These characteristics make red mud a potentially dangerous waste product. Therefore, its safe and cost-effective disposal is currently a pressing issue¹⁴.

* Corresponding author: aldo.boccaccini@ww.uni-erlangen.de

Soda lime glass cullet (G) from urban waste collection services needs to be washed, treated and ground to clean it and remove contaminants like plastic and ceramic. Although this “closed loop recycling” has been implemented in the last years, it has not been possible to reuse all glass fractions in the glass industry¹⁵. Indeed, the impurities are concentrated in glass particles under 100 μm , which could generate foaming problems in an industrial furnace. For this reason, this fraction is currently land-filled. In this investigation, the fly ash used in the production of geopolymers was substituted with 10, 20 and 30 wt% glass waste or red mud to study the possibility of creating new inorganic polymers incorporating a combination of problematic wastes. Bobirica *et al.*¹⁶ and Novais *et al.*¹⁷ have already evaluated the possibility of incorporating different amounts of spent fluorescent lamp waste in geopolymer structures. Their studies have determined a decrease in the mechanical properties with an increasing amount of glass added. Similarly, the incorporation of different amounts of red mud during geopolymer synthesis was determined by Kuman *et al.*¹⁸ and Mucsi *et al.*¹⁹ to affect negatively the geopolymers’ performance. The influence of the addition of waste materials on the structural and mechanical properties of the produced geopolymers was evaluated.

II. Materials and Methods

(1) Characterization of raw materials

Low-calcium fly ash (Class F according to ASTM C618), red mud and waste glass were used in this investigation. Fly ash with a mean particle size of 37 μm was provided by Steag power mineral GmbH, Dinslaken, Germany. The waste glass is a soda lime glass with particle size under 60 μm obtained from Sasil S.p.A Biella, Italy, while red mud with a particle size under 75 μm was collected by Alteo, Gardanne, France.

The chemical composition of the raw materials was determined by means of X-ray fluorescence analysis (XRF) with a Spectro Xepos He energy-dispersive X-ray fluorescence spectrometer (Spectro Analytical Instruments GmbH). For the analyses, fusion tablets were fabricated by adding 4.830 g $\text{Li}_2\text{B}_4\text{O}_7$ and 230 mg I_2O_5 as flux to 1 g of sample powder. An Oxiflux fusion system (CRB Analyse Service GmbH) was used for fusion tablet fabrication. The results are given in Table 1.

The quantitative phase composition of the raw materials was determined by means of powder X-ray diffraction (XRD) combined with Rietveld refinement and the G-factor method²⁰. XRD measurements were performed with a D8 Advance with DaVinci design diffractometer (Bruker AXS). The following measurement parameters were applied: range: 7° – 70° 2 θ ; step size: 0.01125° 2 θ , integration time: 0.4 s; radiation: copper K α ; generator settings: 40 mA, 40 kV; divergence slit: 0.3°. Three independent preparations were measured for fly ash and glass. Red mud was analysed five times because the quantification of some phases was less reproducible in this sample.

Table 1: Chemical composition of raw materials (wt%) determined with XRF.

Constituent	Fly ash	Red mud	Glass
SiO ₂	54.36	5.21	70.50
TiO ₂	1.07	8.05	0.07
Al ₂ O ₃	24.84	15.21	3.20
Fe ₂ O ₃	8.28	52.94	0.42
MnO	0.009	0.05	-
MgO	2.06	0.38	2.3
CaO	2.56	2.95	10.00
Na ₂ O	0.83	2.40	12.00
K ₂ O	3.03	0.63	1.00
P ₂ O ₅	0.38	0.54	-
Loss	2.10	10.77	0.40
on ignition			

Rietveld refinement was performed with the software TOPAS 4.2 (Bruker AXS).

The G-factor method, an external standard method, was applied to obtain the absolute contents of crystalline phases. Details of the method can be found in reference²⁰. The amorphous content of the samples could be determined as the difference of the sum of all crystalline phases quantities to 100 wt%. The G-factor, which is a device-specific calibration constant, was obtained by measuring a quartzite slice (fine-grained rock of almost pure quartz) as an external standard under identical measurement conditions as for the samples. The quartzite was prior calibrated with pure crystalline silicon powder, NIST Si Standard 640d. The mass attenuation coefficients (MACs) of the powder samples were determined from the chemical composition obtained with the XRF data and the MACs of the elements presented in reference²¹. Quantitative phase composition of fly ash, red mud and glass, determined with the G-factor method are shown in Tables 2, 3 and 4.

Table 2: Quantitative phase composition of fly ash, determined with G-factor method. The structures given in the references for each phase were used for Rietveld refinement.

Mineral	Formula	Fly Ash [wt%]
Mullite ²²	3Al ₂ O ₃ ·2SiO ₂	18.5 ± 0.4
Quartz ²³	SiO ₂	17.2 ± 0.3
Hematite ²⁴	Fe ₂ O ₃	2.08 ± 0.07
Magnetite ²⁵	Fe ₃ O ₄	1.64 ± 0.06
Anhydrite ²⁶	CaSO ₄	0.88 ± 0.08
Periclase ²⁷	MgO	0.44 ± 0.02
Lime ²⁸	CaO	0.24 ± 0.02
Amorphous fraction	-	59.0 ± 0.9

The reproducibility of the three independent fly ash measurements was satisfactory. Fly ash is mainly composed of an amorphous fraction (59.0 ± 0.9 wt%). The main crystalline phases of fly ash are mullite and quartz (Table 2.)

The mineralogical composition of red mud is rather complex, with goethite and hematite as the main mineral phases (Table 3). The quantification of some minor phases was not sufficiently reproducible. The reason might be an inhomogeneous distribution of these minerals in the sample. The amorphous fraction of red mud is rather low. As expected, the glass is characterized by a highly predominant amorphous phase (96.1 ± 0.6 wt%) (Table 4).

Table 3: Quantitative phase composition of red mud, determined with the G-factor method. The structures given in the references for each phase were used for Rietveld refinement.

Mineral	Formula	Red Mud [wt%]
Goethite ²⁹	FeO(OH)	30.7 ± 0.80
Hematite ²⁴	Fe ₂ O ₃	24.5 ± 0.4
Cancrinite ³⁰	Na ₈ (AlSiO ₄) ₆ (CO ₃)(H ₂ O) ₂	10.2 ± 0.6
Gibbsite ³¹	Al(OH) ₃	6.6 ± 0.9
Boehmite ³²	AlO(OH)	6.5 ± 0.2
Rutile ³³	TiO ₂	3.9 ± 0.3
Larnite ³⁴	Ca ₂ SiO ₄	3.4 ± 0.2
Carnegieite ³⁵	NaAlSiO ₄	2.8 ± 0.5
Muscovite ³⁶	K[Al ₂ (OH) ₂ /AlSi ₃ O ₁₀]	1.1 ± 0.6
Amorphous fraction	-	7 ± 5

Table 4: Quantitative phase composition of waste glass, determined with the G-factor method. The structures given in the references for each phase were used for Rietveld refinement.

Mineral	Formula	Glass [wt%]
Quartz ²³	SiO ₂	1.3 ± 0.2
Albite ³⁷	NaAlSi ₃ O ₈	0.9 ± 0.2
Microcline ³⁸	K(AlSi ₃ O ₈)	1.1 ± 0.2
Calcite ³⁹	CaCO ₃	0.30 ± 0.02
Amorphous fraction	-	96.1 ± 0.6

In geopolymerization, the amorphous content plays a predominant role, since it is usually the most reactive source. For instance, the high percentage of amorphous phase in fly ash is one of the reasons why this material is highly suitable for the production of geopolymers^{40, 41}.

(2) Sample preparation

Sodium hydroxide solution (8M) was prepared by dissolution of NaOH pellets (Merk 99.5 %) in distilled water, the waterglass solution (PQ Corporation) has modulus (SiO₂/Na₂O ratio) = 2.0, density at 20 °C = 1.4 g/cm³ and viscosity at 20 °C = 200 mPa.

The final alkaline solution was prepared by mixing Na₂SiO₃ and NaOH solutions with a ratio of 2.5. This solution was prepared one day before the use to allow the exothermically heated solution to cool down to room temperature⁴².

Geopolymer samples were prepared by mixing fly ash, red mud, glass and alkaline solution with a head stirrer at 85 rpm until a homogeneous slurry was obtained. After mechanical mixing, a vibrating table was used to remove entrained air from the slurry before this was cast in polyethylene molds and sealed from the atmosphere. The cylindrical mold had a diameter of 14 mm and height of 31.5 mm. Samples were cured in a laboratory oven at 60 °C for 24 h. After curing, the samples were maintained at room temperature until they were mechanically tested. One mixture was produced using only fly ash as reference material while the other six mixtures were produced by replacing 10 wt%, 20 wt% and 30 wt% of fly ash with waste glass in three batches and with red mud in the other three batches. The details of the mixture proportions used are shown in Table 5.

Table 5: Summary of mixture proportions, liquid-to-solid ratio and sodium silicate solution to sodium hydroxide solution proportion.

Mixture	Fly ash (wt%)	Glass (wt%)	Red mud (wt%)	Liq./Sol.	Waterglass sln./NaOH sln.
FA	100	-	-	0.4	2.5
10G	90	10	-	0.4	2.5
20G	80	20	-	0.4	2.5
30G	70	30	-	0.4	2.5
10RM	90	-	10	0.4	2.5
20RM	80	-	20	0.4	2.5
30RM	70	-	30	0.45	2.5

(3) Testing procedure

The compressive strength of cylindrical samples (height twice the diameter) was measured by using a universal testing machine (Zwick Roell, Ulm, Germany, Series Z050). A minimum of 10 samples for each batch were tested to evaluate the 28-days strength of the specimens.

In addition, three-point bending strength tests and chevron notch for fracture toughness determination tests were carried out using a Zwick/Roell Z50 machine. Ten specimens, with the geometry 4 × 3 × 20 mm³ and a minimum span length of 16 mm, were tested for each sample type. The samples were cut and ground under dry conditions. For flexural strength determination, the specimens were loaded in three-point bending at a constant cross-head speed of 10 μm/min at room temperature. The flexural strength (σ) was calculated using the following equation⁴³:

$$\sigma = \frac{3FL}{2BW^2} \tag{1}$$

where F is the fracture load, L is the span length, B the width and W the height of the specimen⁴⁴.

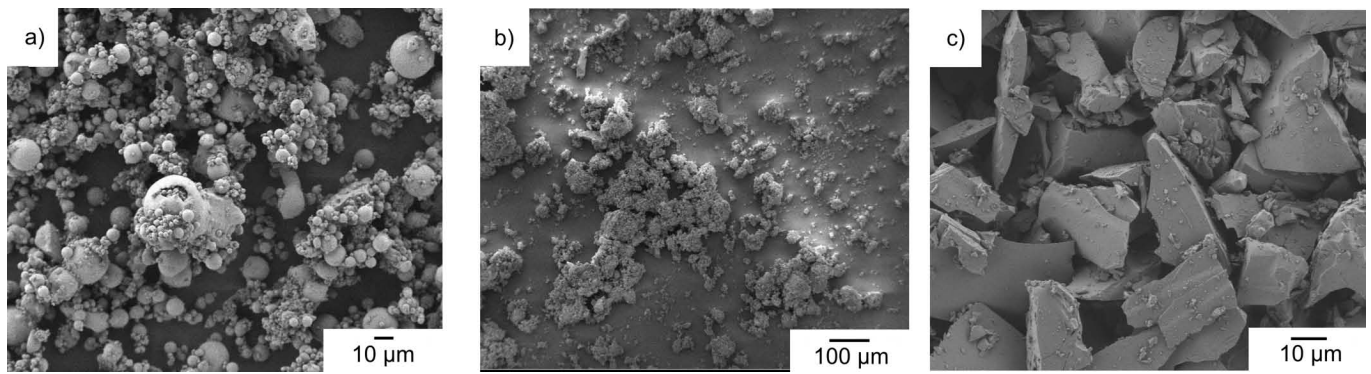


Fig. 1: SEM images of raw materials used to prepare geopolymers: (a) fly ash, (b) red mud (c) recycled glass.

To determine the fracture toughness the chevron notch technique was used according to the methodology described in refs.^{45, 46}. The fracture toughness (K_{IC}) was calculated with the following equation:

$$K_{IC} = \frac{Y_{min}^* F_M}{B W^{1/2}} \quad (2)$$

where Y_{min}^* is a minimum of the geometrical compliance function, F_M is the maximum load, which was obtained from load deflection traces as the maximum flexural load. The tests were carried out at room temperature; the cross-head speed applied was 0.5 mm/min.

A qualitative microstructural evaluation of the raw materials and final geopolymer samples was performed by means of scanning electron microscopy (LEO 435 VP, LEO Electron Microscopy Ltd., Cambridge, UK and Ultra Plus, Zeiss, Jena, Germany) in order to evaluate the homogeneity of the glass and red mud incorporated in the geopolymer matrix. Pieces of samples after compression strength test were used to analyze the microstructure.

Fourier transform infrared (FTIR) spectra were recorded using a Nicolet 6700 device in the range between 4000 cm^{-1} and 400 cm^{-1} . The specimens for FTIR were prepared using the KBr pellet technique.

III. Results and Discussion

(1) Micromorphology of raw materials

From SEM images (Fig. 1) it can be observed that the morphology of fly ash (Fig. 1a) is mainly composed of (hollow) spherical particles of different dimensions bonded together. The irregularly shaped particles are probably derived from unburned particles or agglomerated minerals⁴⁷. The red mud particles in Fig. 1b are flake-shaped with visible agglomerates even after sieving. The recycled soda lime glass powder consists of a heterogeneous distribution of irregularly shaped, smooth fragments (Fig. 1c).

(2) Compressive strength

For each mixture, ten samples were tested to evaluate the compressive strength after 28 days aging and the results are shown in Fig. 2.

The geopolymers prepared using only fly ash as raw material exhibited the highest compressive strength, with a value of 75 ± 14 MPa. Cement with a compressive strength up to 70 MPa is classified as a high-strength material⁴⁸. The

results presented in Fig. 2 show the same trend in strength development after the addition of red mud or recycled glass. The addition of both raw materials caused the compressive strength to decrease, as the amount of recycled glass and red mud added to the mixture increased. In particular, the mixture containing 20 wt% recycled glass displayed the lowest mechanical strength, with a reduction of 40 %.

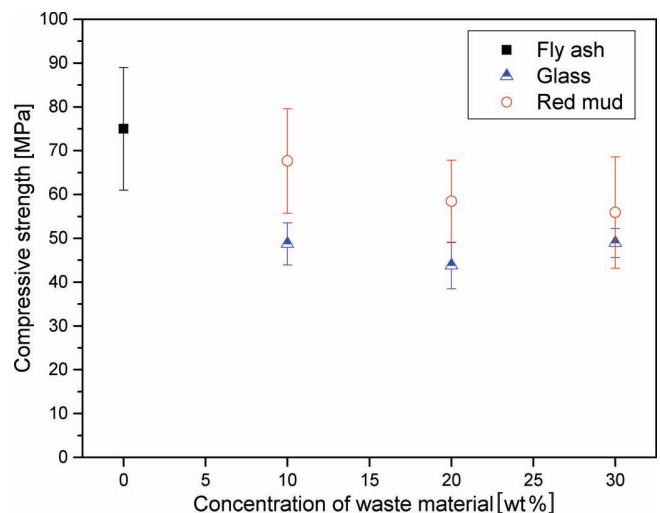


Fig. 2: Compressive strength of fly-ash-based geopolymers with an addition of 10, 20, and 30 wt% of glass or red mud after 28 days of aging.

Except for the 10 wt% substitution, where the introduction of recycled glass affects the compressive strength considerably compared with red mud, for the other percentages the compressive strength values were in the same range.

Many authors agree that a higher red mud content leads to overall lower compressive strengths of geopolymer samples⁴⁹. For example Kumar *et al.*¹⁸, Zhang *et al.*⁵⁰, Mucsi *et al.*¹⁹, He *et al.*⁴⁹ demonstrated that with a ratio of 80 : 20 fly ash to red mud, a maximum value of approx. 25 MPa can be achieved and increasing the red mud amount over 20 % causes a drastic decrease in the compressive strength of the material. In the present case, Fig. 2 shows that there is no significant difference in compressive strength with the addition of 20 or 30 wt% red mud to the original mixture, moreover in both cases the mechanical strength values remain close to a satisfactory value of 60 MPa.

Owing to the high amount of silica in the glass and of alumina in red mud, it is expected that the initial $\text{SiO}_2/\text{Al}_2\text{O}_3$ molar ratio will increase as the amount of glass rises and decrease when red mud is added to the geopolymer. Si-O-Si bonds are stronger than Si-O-Al and Al-O-Al bonds, for this reason a geopolymer richer in silica than in aluminum could exhibit a better mechanical performance¹⁶. SEM images showed, however, that the glass particles were not completely integrated inside the structure (see Fig. 7), which could explain the lower mechanical strength of the glass-containing samples.

Moreover, the addition of glass to the system requires a higher amount of water, resulting in the formation of relatively large cracks and higher shrinkage. Different authors have already tested the possibility of incorporating glass waste in alkaline-activated matrices⁵¹. Introduction of waste glass into fly-ash-based geopolymers causes a decrease in their mechanical properties as confirmed from the literature. For example, Bobirica *et al.*¹⁶ and Novais *et al.*¹⁷ determined a decrease of up to 55 % in mechanical strength after introducing 10 and 20 wt% fluorescent lamp glass waste, with a maximum value of 19 MPa. With the introduction of soda lime glass, a decrease close to 45% was observed in this study, but the strength remained at a satisfactory value of 50 MPa.

Therefore, it can be concluded that the compressive strength of the fly-ash-based geopolymers with red mud and waste glass in the range (45–60 MPa) was lower than that of pure fly ash geopolymer (75 MPa), but is still satisfactory in comparison with the results in the literature.

(3) Flexural strength

The flexural strength test is one of the most common tests conducted on hardened concrete, this determines the load at which structural elements crack. The flexural properties were measured in a 3-point bending test of beams having cross-section of $3 \times 4 \text{ mm}^2$. In Fig. 3, typical load-deflection curves for the samples with fly ash, fly ash plus waste glass (10 wt%) and fly ash plus red mud (10 wt%) are plotted. The curves show a linear behavior until brittle fracture occurs followed by a sudden drop in load when the fracture strength was reached. Different slopes of the linear part, even though affected by the real cross-section area of samples, reflect differences in the Young's modulus of the materials.

In Fig. 4, average values of the flexural strength are plotted for geopolymers made with pure fly ash and geopolymers containing glass or red mud. The effect of glass addition in comparison to red mud addition on the flexural strength is quite different. While the incorporation of waste glass has a negative effect in terms of flexural strength, the addition of red mud provides a slight improvement in flexural strength related to fly-ash-only geopolymers from $11 \pm 2 \text{ MPa}$ to $15 \pm 2 \text{ MPa}$. Moreover, a relatively high value of flexural strength is maintained nearly constant up to a high incorporation of red mud (30 wt%).

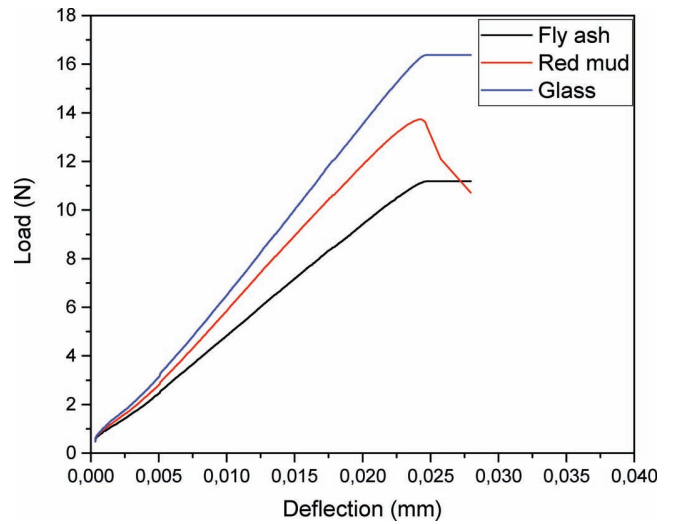


Fig. 3: Load-deflection curves for the different geopolymers investigated.

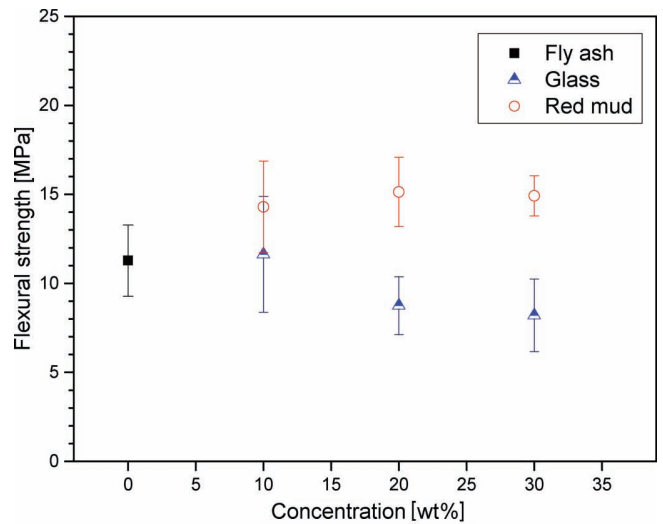


Fig. 4: Average of the flexural strength for all samples investigated.

(4) Fracture Toughness

The fracture toughness quantified with the critical stress intensity factor (K_{IC}), determined from the chevron notch tests, indicates the level of the stress concentration at the crack tip needed for crack initiation from the notch¹². The K_{IC} was calculated for 10 samples of each batch using Equation (2). The notch depth, necessary for the calculation, was measured using image analysis software from optical microscope images. Examples of macrographs of fracture surfaces are shown in Fig. 5.

The fracture toughness values shown (in Fig. 6) for each geopolymer sample are the average between the two values calculated from the two parts of the same sample obtained after rupture. For most of the samples, the K_{IC} value from the right and left parts of the specimen was the same, just for a few samples there was a minimal variation in the value, probably due to differences in the fracture performance and inaccuracy during the measurements.

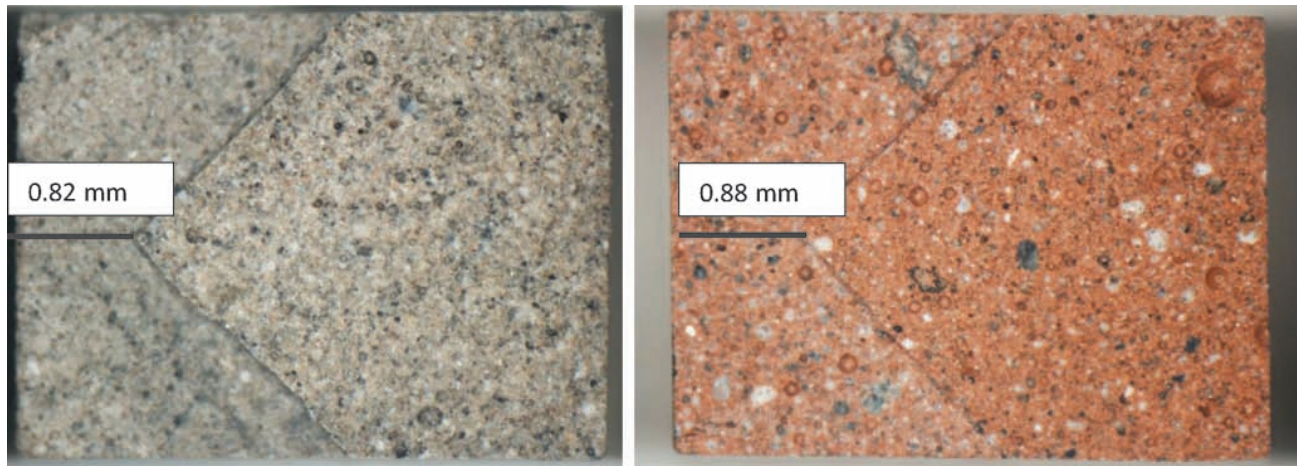


Fig. 5: Notch depth determined in a sample containing 20 wt% glass (left) and 10 wt% red mud (right).

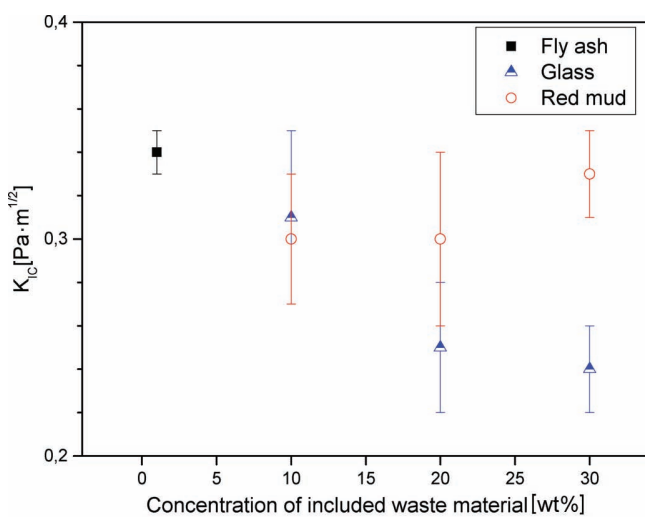


Fig. 6: Mean fracture toughness values of the different geopolymers investigated.

The statistic test carried out using ten samples for each composition demonstrated a high homogeneity in K_{IC} values with low variability. This result indicates that the measurements are highly reproducible. The low scattering of K_{IC} values might have been caused by some porosity and the intrinsic microstructural inhomogeneity of samples. The averages of the fracture toughness values for each batch are summarized in Fig. 6.

The fracture toughness does not change significantly with substitution of part of the fly ash with soda lime glass or red mud. From the figure, it is evident that all values are lying in the range between 0.25 and 0.35 MPa·m^{1/2}. However, increasing soda lime glass content seems to reduce K_{IC} to a higher extent, while the introduction of red mud does not affect the fracture toughness. This result can be explained considering that an increase of the waste glass content could result in a microstructure with a higher concentration of defects and cracks. Even if the presence of non-reacted glass particles could deflect cracks, hindering their propagation, this effect was insufficient to balance the negative effect of porosity and cracks already present in the matrix. Moreover both dissolution and polycondensation, the main steps of geopolymerization, are heterogeneous processes, in which it is difficult to control

the final uniformity of the matrix⁵². On the other hand, geopolymers incorporating red mud are expected to exhibit an ultimately more homogeneous structure than that of glass-containing geopolymers, which can explain the improvement in fracture toughness.

(5) Scanning electron microscopy

Scanning electron microscopy (SEM) was used to evaluate the microstructure of each geopolymer batch. Fig. 7 shows SEM images of geopolymer specimens containing 10, 20 or 30 wt% soda lime glass or red mud at the same magnification. Geopolymers are mostly composed of fly ash containing a significant amount of hollow spheres. When these spheres partially dissolve, they create porosity in the matrix and un-reacted particles can be found in hollow cavities, as shown in Fig. 7. The porosity probably results from the spaces left after fly ash dissolution or water evaporation during the curing process.

The micrographs of geopolymers containing recycled glass show unreacted glass particles and fly ash in the likely amorphous geopolymer matrix. In particular, increasing the amount of glass leads to significant formation of relatively large cracks and pores, which are larger than those after the addition of red mud; particularly at 30% loading.

It is likely that glass requires more water from the system compared to fly ash and red mud. As a consequence, the final geopolymer will incur higher shrinkage with subsequent reduced interface adhesion between the initial raw phases. The amount of dissolved silica and alumina, as mentioned before, correlates with the amorphous fraction in the raw materials. It is indeed not expected that all glass particles inside the geopolymer would dissolve taking part in the geopolymerization process. This is confirmed by the glass particles visible in the microstructure. Moreover, with an increase in the amount of glass, the amount of unreacted silica should increase, in particular if the reaction product covers the glass particles, making it more difficult for them to dissolve inside the alkali solution. Particle size is a key factor in glass solubility⁵³, as has been extensively documented in the literature. Torres Carrasco *et al.*⁵³ and Cyr *et al.*⁵⁴ for example, tested the influence of glass

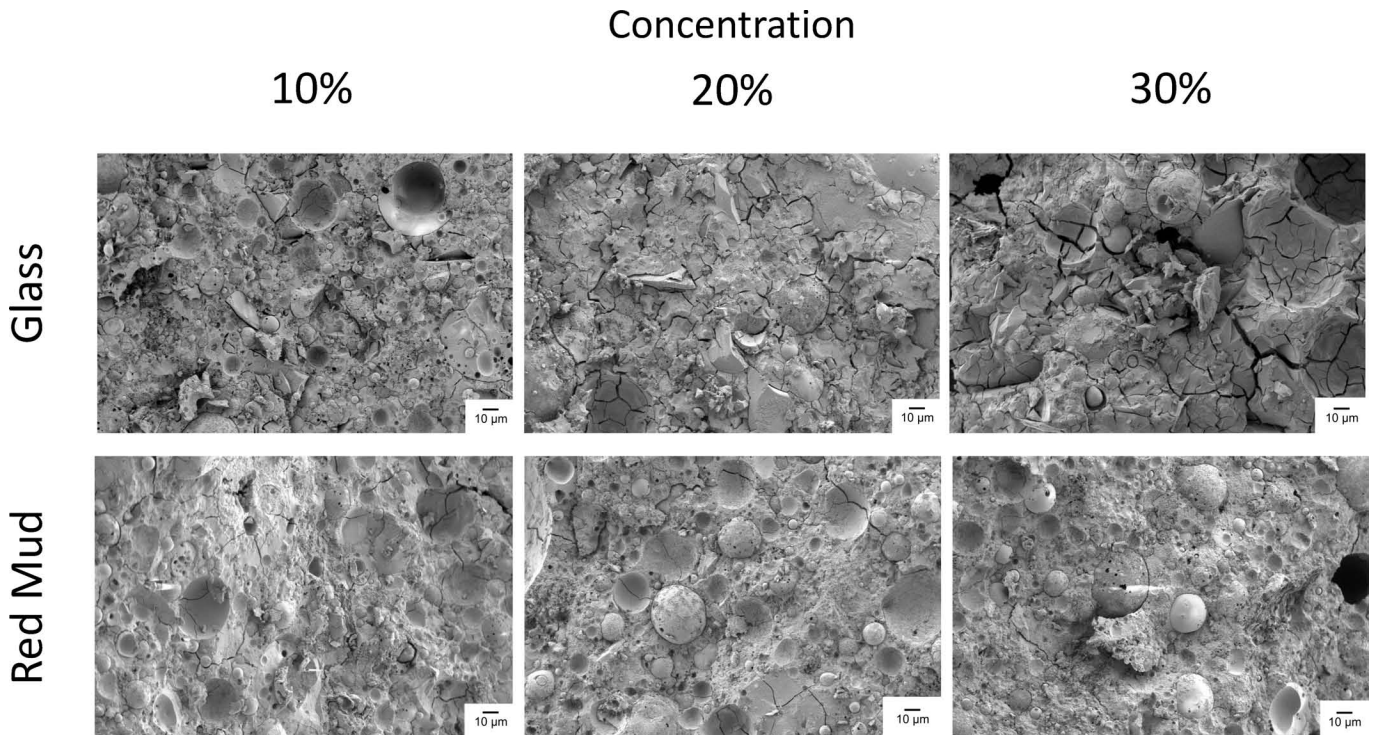


Fig. 7: SEM images of geopolymer fracture surfaces after compression strength tests with different substitution level of recycled glass (G) or red mud (RM).

granulometry in geopolymerization. The results showed that the lower the particle size range, the higher the compressive strength was. In particular, reducing the fineness from 75 μm to 15 μm for the average grain size was shown to lead to an increase in the mechanical strength by up to five times its original value⁵⁴.

In this study, the solubility could also be improved by decreasing the particle size of the glass, however, this implies introducing pretreatment of the raw materials (recycled glass) before the raw materials are reacted. For economic and environmental reasons, soda lime glass waste and red mud should be used directly as received from waste processing facilities.

The SEM images reveal a denser structure of geopolymer specimens incorporating red mud, this is consistent with the measured compressive strength values (Fig. 2). Red mud consists of particles that have a good capacity to assemble together, filling the spaces left by fly ash particles upon their dissolution and leading to a compact final microstructure. The micrographs shown in Fig. 7 indicate that increasing the amount of red mud does not affect the mesostructural homogeneity of the final geopolymer.

(6) IR Spectroscopy

The FTIR spectra in Fig. 8 show the same trend for mixtures containing red mud and recycled glass. Peaks at 453 cm⁻¹ and 455 cm⁻¹ belong to Si-O respectively Si-O-Si bending vibration¹.

The small bands between 790 and 800 cm⁻¹ are attributed to the bands present in the fly ash source as quartz or mullite^{16, 55}. The main absorption band is located between 900 and 1100 cm⁻¹, which is attributed to the Si-O-Al and Si-O-Si asymmetric stretching vibrations. The peak at 555 cm⁻¹ is assigned to the Si-O-Al bending vibration,

this peak is more intense for geopolymers containing red mud, thanks to the high amount of alumina, as this promotes its formation.

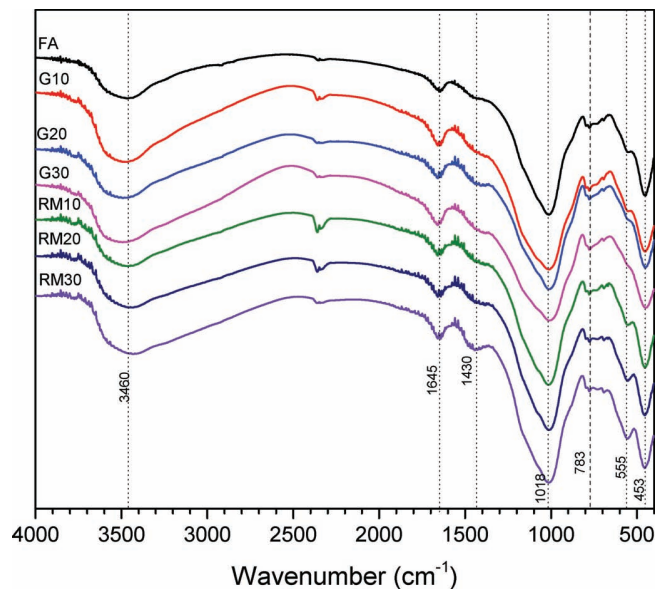


Fig. 8: FTIR spectra of geopolymer based on fly ash and geopolymers with 10, 20 and 30% of glass or red mud.

The peak identified at 1430 cm⁻¹ can be related to the O-C-O stretching vibration of a carbonate phase, which might be formed from remaining unreacted activator and CO₂⁵⁶. Peaks at 3390–3370 cm⁻¹ are related to -OH, H-O-H bonds stretching vibration, while the peak between 1600 cm⁻¹ and 1650 cm⁻¹ corresponds to the H-O-H bending vibration. Since these bands are generated by water molecules, they are an indicator of the hydration

of the geopolymer^{19,55}. Fig. 8 evidences how the incorporation of glass waste and red mud did not inhibit the formation of an aluminosilicate gel, but only changed the intensity of the peaks related to the X-O vibration, where X is Al or Si.

IV. Conclusions

This study investigated the behavior of geopolymers based on the combination of fly ash with recycled soda lime glass or red mud, with a particular focus on the variations in the mechanical behavior. The introduction of recycled glass causes only a slight decrease in the flexural strength in comparison to that of the geopolymer prepared only with fly ash, the decrease in K_{IC} is more pronounced.

Nevertheless, the incorporation of waste glass or red mud leads, in general, to structurally sound materials with satisfactory properties for different fields of applications.

Summing up the results from mechanical tests and microstructural analysis, we can conclude that the loss of compressive strength in glass-modified geopolymers relates to the presence of remaining unreacted glass particles and micro-crack development. On the other hand, the replacement of fly ash with red mud produces a negligible decrease in mechanical properties. The results of the bending test indicate no substantial differences originating from the substitution of fly ash with the other by-products. Moreover, red mud addition seems to have a better influence on fracture toughness and flexural strength compared to waste glass incorporation. In conclusion, fly ash in geopolymer technology can be substituted with waste glass or red mud without drastically modifying the final properties, which remain within the ranges required in construction applications. The present approach thus represents a new novel end-use for these waste products.

Acknowledgments

The authors gratefully acknowledge the support of the European Union's Horizon 2020 research and innovation programme under the Marie Skłodowska-Curie grant agreement No. 642557 (Project CoACH).

References

- Davidovits, J.: Geopolymer chemistry & applications. 3rd edition. Geopolymer Institute, 2011.
- Liew, Y.M., Kamarudin, H., Al Bakri, A.M., Bnhussain, M., Luqman, M., Nizar, I.K., Ruzaidi, C., Heah, C.: Optimization of solids-to-liquid and alkali activator ratios of calcined kaolin geopolymeric powder, *Constr. Build. Mater.*, **37**, 440–451, (2012).
- Verdolotti, L., Iannace, S., Lavorgna, M., Lamanna, R.: Geopolymerization reaction to consolidate incoherent pozzolanic soil, *J. Mater. Sci.*, **43**, 865–873, (2008).
- Okoye, F., Durgaprasad, J., Singh, N.: Effect of silica fume on the mechanical properties of fly ash based-geopolymer concrete, *Ceram. Int.*, **42**, 3000–3006, (2016).
- Bondar, D.: Geo-polymer concrete as a new type of sustainable construction materials. In: Proceedings of the Third International Conference on Sustainable Construction Materials and Technologies, Coventry University and The University of Wisconsin Milwaukee Centre for By-products Utilization (2013).
- Zhu, P., Kai, G., Kenan, F., Sanjayan, J.G., Duan, W., Collins, F.G.: Damping capacity of fly ash-based geopolymer. ICCM 2011: Proceedings of the 18th International Conference on Composite Materials. Springer, 2013.
- Al Muhit, B., Foong, K., Alengaram, U., Jumaat, M.Z.: Geopolymer Concrete: A building material for the future, *Electr. J. of Struct. Eng.*, **13**, [1], (2013).
- Xu, H., Van Deventer, J.: The geopolymerisation of aluminosilicate minerals, *Int. J. Miner. Process*, **59**, 247–266, (2000).
- Kupaei, R.K., Alengaram, U.J., Jumaat, M.Z.: The effect of different parameters on the development of compressive strength of oil palm shell geopolymer concrete, *Sci. World J.*, **2014**, 898536, (2014).
- Kriven, W.M.: Inorganic polysialates or “Geopolymers”, *Am. Ceram. Soc. Bull.*, **89**, [4], 31–34, (2010).
- Sankar, K., Kriven, W.M.: Geopolymer reinforced with E-glass leno weaves, *J. Am. Ceram. Soc.*, **100**, 2492–2501, (2017).
- Sarker, P.K., Haque, R., Ramgolam, K.V.: Fracture behaviour of heat cured fly ash based geopolymer concrete, *Mater. Des.*, **44**, 580–586, (2013).
- Drechsler, M., Graham, A.: Innovative Materials Technologies: Bringing resource sustainability to construction and mining industries, *Inst. Quarr. Aust. Annu. Conf. Aust.* 1–11, Oct. (2005)
- Zhang, M., El-Korchi, T., Zhang, G., Liang, J., Tao, M.: Synthesis factors affecting mechanical properties, microstructure, and chemical composition of red mud-fly ash based geopolymers, *Fuel*, **134**, 315–325, (2014).
- Rincón, A., Giacomello, G., Pasetto, M., Bernardo, E.: Novel ‘inorganic gel casting’ process for the manufacturing of glass foams, *J. Eur. Ceram. Soc.*, **37**, 2227–2234, (2017).
- Bobiričá, C., Shim, J.-H., Pyeon, J.-H., Park, J.-Y.: Influence of waste glass on the microstructure and strength of inorganic polymers, *Ceram. Int.*, **41**, 13638–13649, (2015).
- Novais, R.M., Ascensão, G., Seabra, M.P., Labrincha, J.A.: Waste glass from end-of-life fluorescent lamps as raw material in geopolymers, *Waste Manage.*, **52**, 245–255, (2016).
- Kumar, A., Kumar, S.: Development of paving blocks from synergistic use of red mud and fly ash using geopolymerization, *Constr. Build. Mater.*, **38**, 865–871, (2013).
- Mucsi, G., Szabo, R., Racz, Á., Molnar, Z., Kristály, F., Kumar, S.: Influence of red mud on the properties of geopolymer derived from mechanically activated lignite fly ash. In: Proceedings of the Bauxite Residue Valorisation and Best Practices Conference, Leuven, (2015).
- Jansen, D., Stabler, C., Goetz-Neunhoeffler, F., Dittrich, S., Neubauer, J.: Does ordinary portland cement contain amorphous phase? A quantitative study using an external standard method, *Powder Diffr.*, **26**, 31–38, (2011).
- Prince, E.: International union for crystallography, international tables for crystallography, Volume C. Mathematical Physical and Chemical Tables, 3rd edition, Wiley, 2004.
- Ban, T., Okada, K.: Structure refinement of mullite by the rietveld method and a new method for estimation of chemical composition, *J. Am. Ceram. Soc.*, **75**, 227–230, (1992).
- Le Page, Y., Donnay, G.: Refinement of the crystal structure of low-quartz, *Acta Crystallogr.*, **B32**, 227–230, (1976).
- Sawada, H.: An electron density study of α -ferric oxide, *Mater. Res. Bull.*, **31**, 141–146, (1996).
- Bragg, W.H.: The structure of magnetite and the spinels, *Nature*, **95**, 561, (1915).
- Kirfel, A., Will, G.: Charge density in anhydrite, CaSO₄, from X-ray and neutron diffraction measurements, *Acta Crystallogr.*, **B 36**, 2881–2890, (1980).
- Sasaki, S., Fujino, K., Takeuchi, Y.: X-ray determination of electron-density distributions in oxides, MgO, MnO, CoO, and NiO, and atomic scattering factors of their constituent atoms, *Proc. Jpn. Acad.*, **55**, 43–48, (1979).

- 28 Shen, C.H., Liu, R.S., Lin, J.G., Huang, C.Y.: Phase stability study of $\text{La}_{1.2}\text{Ca}_{1.8}\text{Mn}_2\text{O}_7$, *Mater. Res. Bull.*, **36**, 1139–1148, (2001).
- 29 Yang, H.X., Ren, L., Downs, R.T., Costin, G.: Goethite, $\alpha\text{-FeO}(\text{OH})$, from single-crystal data, *Acta Cryst.*, **E62**, i250 – i252, (2006).
- 30 Smolin, Y.I., Shepelev, Y.F., Butikova, I.K., Kobayakov, I.B.: The crystal structure of cancrinite, *Kristallografiya*, **26**, 63–66, (1981).
- 31 Saalfeld, H., Wedde, M.: Refinement of the crystal structure of gibbsite, $\text{Al}(\text{OH})_3$, *Z. Kristallogr. - Crystalline Materials*, **139**, 129–135, (1974).
- 32 Farkas, L., Gado, P., Werner, P.E.: The structure refinement of boehmite ($\text{AlO}(\text{OH})$ - γ) and the study of its structural variability based on Guinier-Hägg powder data, *Mater. Res. Bull.*, **12**, 1213–1219, (1977).
- 33 Abrahams, S.C., Bernstein, J.L.: Rutile: normal probability plot analysis and accurate measurement of crystal structure, *J. Chem. Phys.*, **55**, 3206–3211, (1971).
- 34 Jost, K.H., Ziemer, B., Seydel, R.: Redetermination of the structure of β -dicalcium silicate, *Acta Cryst.*, **B33**, 1696–1700, (1977).
- 35 Withers, R.L., Thompson, J.G.: Modulation wave approach to the structural parametrization and rietveld refinement of low carnegieite, *Acta Crystallogr.*, **B49**, 614–624, (1993).
- 36 Gatineau, L.: Localisation of isomorphic substitutions in muscovite, in French, *Comptes Rendus Hebd. Des Séances l'Académie*. **256**, 4648–4649, (1963).
- 37 Phillips, M.W., Colville, A.A., Ribbe, P.H.: The crystal structures of two oligoclases: A comparison with low and high albite, *Z. Kristallogr. - Crystalline Materials*, **133**, [1–6], 43–65, (1971).
- 38 Blasi, A., De Pol Blasi, C., Zanazzi, P.F.: A re-examination of the pellets microcline: mineralogical implications and genetic considerations, *Can. Mineral.*, **25**, 527–537, (1987).
- 39 Maslen, E.N., Streltsov, V.A., Streltsova, N.R.: Electron density and optical anisotropy in rhombohedral Carbonates. III.* synchrotron X-ray studies of CaCO_3 , MgCO_3 and MnCO_3 , *Acta Cryst.*, **B51**, 929–939, (1995).
- 40 Temuujin, J., Williams, R.P., Van Riessen, A.: Effect of mechanical activation of fly ash on the properties of geopolymer cured at ambient temperature, *J. Mater. Process. Technol.*, **209**, [12], 5276–5280, (2009).
- 41 Temuujin, J., Van Riessen, A.: Effect of fly ash preliminary calcination on the properties of geopolymer, *J. Hazard. Mater.*, **164**, [2], 634–639, (2009).
- 42 Liu, M.Y.J., Chua, C.P., Alengaram, U.J., Jumaat, M.Z.: Utilization of palm oil fuel ash as binder in lightweight oil palm shell geopolymer concrete, *Advances in Materials Science and Engineering*, (2014).
- 43 Yang, H., Jiang, L., Zhang, Y., Pu, Q.: Flexural strength of cement paste beam under chemical degradation: experiments and simplified modeling, *J. Mater. Civ. Eng.*, **25**, [5], 555–562, (2012).
- 44 Pernica, D., Reis, P.N.B., Ferreira, J.A.M., Louda, P.: Effect of test conditions on the bending strength of a geopolymer-reinforced composite, *J. Mater. Sci.*, **45**, [3], 744, (2010).
- 45 Dlouhý, I., Boccaccini, A.R.: Reliability of chevron notch technique for fracture toughness determination in glass composites reinforced by continuous fibres, *Scripta Mater.*, **44**, [3], 531–537, (2001).
- 46 Boccaccini, A.R., Rawlings, R.D., Dlouhý, I.: Reliability of the chevron-notch technique for fracture toughness determination in glass, *Mater. Sci. Eng. A*, **347**, [1], 102–108, (2003).
- 47 Ziegler, D., Formia, A., Tulliani, J.M., Palmero, P.: Environmentally-friendly dense and porous geopolymers using fly ash and rice husk ash as raw materials, *Materials*, **9**, [6], 466, (2016).
- 48 Aitcin, P.C.: High-performance concrete demystified, *Concrete International*, **15**, [1], 21–26, (1993).
- 49 He, J., Zhang, G.: Geopolymerization of red mud and fly ash for civil infrastructure applications. In: *Geo-Frontiers 2011: Advances in Geotechnical Engineering*, 1287–1296, (2011).
- 50 Zhang, M., El-Korchi, T., Zhang, G., Liang, J., Tao, M.: Synthesis factors affecting mechanical properties, microstructure, and chemical composition of red mud-fly ash based geopolymers, *Fuel*, **134**, 315–325, (2014).
- 51 Kourti, I., Rani, D.A., Deegan, D., Boccaccini, A.R., Cheeseman, C.R.: Production of geopolymers using glass produced from DC plasma treatment of air pollution control (APC) residues, *J. Hazard. Mater.*, **176**, [1], 704–709, (2010).
- 52 Kamseu, E., Bignozzi, M. C., Melo, U. C., Leonelli, C., Sglavo, V.M.: Design of inorganic polymer cements: Effects of matrix strengthening on microstructure, *Constr. Build. Mater.*, **38**, 1135–1145, (2013).
- 53 Torres-Carrasco, M., Palomo, J.G., Puertas, F.: Sodium silicate solutions from dissolution of glasswastes. statistical analysis, *Mater. Construcc*, **64**, [314], 014, (2014).
- 54 Cyr, M., Idir, R., Poinot, T.: Properties of inorganic polymer (geopolymer) mortars made of glass cullet, *J. Mater. Sci.*, **47**, [6], 2782–2797, (2012).
- 55 Rosas-Casarez, C.A., Arredondo-Rea, S.P., Gómez-Soberón, J.M., Alamaral-Sánchez, J.L., Corral-Higuera, R., Chinchillas-Chinchillas, M.J., Acuña-Agüero, O.H.: Experimental study of XRD, FTIR and TGA techniques in geopolymeric materials. In: *Proceedings of the International Conference on Advances in Civil and Structural Engineering – CSE*, 2014.
- 56 Lin, K.L., Shiu, H.S., Shie, J.L., Cheng, T.W., Hwang, C.L.: Effect of composition on characteristics of thin film transistor liquid crystal display (TFT-LCD) waste glass-metakaolin-based geopolymers, *Constr. Build. Mater.*, **36**, 501–507, (2012).

